



HAL
open science

Specific energy requirement of direct contact membrane distillation

Waritha Jantaporn, Aamer Ali, Pierre Aimar

► **To cite this version:**

Waritha Jantaporn, Aamer Ali, Pierre Aimar. Specific energy requirement of direct contact membrane distillation. *Chemical Engineering Research and Design*, 2017, 128, pp.15-26. 10.1016/j.cherd.2017.09.031 . hal-01889877

HAL Id: hal-01889877

<https://hal.science/hal-01889877>

Submitted on 8 Oct 2018

HAL is a multi-disciplinary open access archive for the deposit and dissemination of scientific research documents, whether they are published or not. The documents may come from teaching and research institutions in France or abroad, or from public or private research centers.

L'archive ouverte pluridisciplinaire **HAL**, est destinée au dépôt et à la diffusion de documents scientifiques de niveau recherche, publiés ou non, émanant des établissements d'enseignement et de recherche français ou étrangers, des laboratoires publics ou privés.



Open Archive Toulouse Archive Ouverte

OATAO is an open access repository that collects the work of Toulouse researchers and makes it freely available over the web where possible

This is an author's version published in: <http://oatao.univ-toulouse.fr/20407>

Official URL: <https://doi.org/10.1016/j.cherd.2017.09.031>

To cite this version:

Jantaporn, Waritha^{ORCID} and Ali, Aamer and Aimar, Pierre^{ORCID} *Specific energy requirement of direct contact membrane distillation.* (2017) *Chemical Engineering Research and Design*, 128. 15-26. ISSN 0263-8762

Any correspondence concerning this service should be sent to the repository administrator: tech-oatao@listes-diff.inp-toulouse.fr

Specific energy requirement of direct contact membrane distillation

Waritha Jantaporn^a, Aamer Ali^b, Pierre Aimar^{a,*}

^a Laboratoire de Génie Chimique, Université de Toulouse, CNRS, INPT, UPS, Toulouse, France

^b Institute on Membrane Technology, National Research Council, Cubo 17C, Via Pietro BUCCI, 87036 Rende, CS, Italy

A B S T R A C T

The study aims to provide a clear picture of the thermal energy requirements of Direct Contact Membrane Distillation (DCMD) system as function of different variables influencing the specific energy consumption. This includes membrane properties, operating conditions, recovery factor and the option of heat recovery from the permeate and retentate streams. We simultaneously analyze the variation in specific energy demand and membrane surface area needed as a function of the membrane characteristics, operating conditions and recovery rate, taken as a design parameter. We observe that the specific energy demand of DCMD shows a relatively weak dependence on temperature polarization and membrane properties considered in the current study and a strong dependence on the recovery rate. The advantages of using a heat exchanger very much depends on the recovery rate of the process.

1. Introduction

Membrane processes significantly contribute to modern desalination and wastewater treatment sectors. In addition to the conventional processes (ultrafiltration, microfiltration, nanofiltration, reverse osmosis, electrodialysis, etc.), relatively new processes with different separation potential, driving force and energy consumption are gaining interest. Membrane distillation (MD) is a prominent example of the latter. The process uses a vapor pressure difference, created across a microporous hydrophobic membrane mainly through a temperature difference, as a driving force. It offers the benefit of using low grade heat to induce the required driving force and can treat highly concentrated solutions such as reverse osmosis brines. Due to theoretical 100% rejection of all nonvolatile components, the product is of very high purity.

For a given feed, the performance of MD is mainly dependent upon membrane characteristics and process variables (operating conditions, module characteristics, applied configuration, etc.). High permeability, high liquid entry pressure (LEP), stable hydrophobic character and low thermal conductivity are the main requisites for MD membranes. In order to incorporate these features, membranes with different porosities, pore sizes, materials and hydrophobic characteristics have been

fabricated, making it interesting to compare the process performance of these membranes with commonly used commercial membranes prepared for other separation purposes. Process design improvements in MD mainly focus on improving heat and mass transfer (Yang et al., 2011a; Ali et al., 2015; Phattaranawik et al., 2001) and energy recovery (Geng et al., 2014; Lin et al., 2014). Temperature polarization (TP), defined as the difference in bulk and membrane surface temperatures, plays an important role in governing heat and mass transport across the membrane (Ali et al., 2013). In DCMD, a temperature polarization is observed on the feed side (the temperature at the interface is lower than in the bulk because of the solvent vaporization and heat conduction through the membrane) and on the distillate side as well (the temperature at the interface is higher than in the bulk due to transfer of heat from feed side by condensation and heat conduction from the retentate compartment). Various experimental and theoretical approaches have been reported to quantify TP in MD (Ali et al., 2013; Gryta et al., 1997; Gryta and Tomaszewska, 1998; Phattaranawik et al., 2003; Tamburini et al., 2013), showing that the quantitative effect of temperature polarization on the overall process performance must be accounted for.

To better analyze the true commercial potential of MD, besides technical aspects, economical standing position of the process must

Nomenclature

Symbols

B	Membrane distillation coefficient of membrane, $\text{kg/m}^2 \text{ s Pa}$
C_{pF}	Feed specific heat, J/kgK
C_{pDi}	Distillate specific heat at the module inlet, J/kgK
C_{pDo}	Distillate specific heat at the module outlet, J/kgK
C_{pR}	Retentate specific heat, J/kgK
E	Efficiency of the external heat exchanger used
E_p	Specific energy consumption per cubic meter of distillate, kWh/m^3
H_v	Water latent heat of vaporization, J/kg
J_w	Theoretical water flux transferred through membrane pores, $\text{kg/m}^2 \text{ s}$
k_g	Thermal conductivity of the gas filling the membrane pores, W/mK
k_p	Thermal conductivity of the material forming the membrane matrix, W/mK
L	Hollow fiber length, m
M	Molecular weight of water, kg/mol
N_{fiber}	Number of hollow fibers required
NUT	Number of transfer units
$P_{c \text{ fiber}}$	Conductive heat flux of one hollow fiber, $\text{J/m}^2/\text{s}$
$P_{c \text{ tot}}$	Total conductive heat flux of hollow fibers, $\text{J/m}^2/\text{s}$
P_{Dm}	Water vapor pressure at the membrane surface of distillate side, Pa
P_e	Total energy flux, $\text{J/m}^2/\text{s}$
P_{Fm}	Water vapor pressure at the membrane surface of feed side, Pa
P_{internal}	Energy to be supplied to the membrane module, $\text{J/m}^2/\text{s}$
P_{tot}	Total heat flux through the membrane, $\text{J/m}^2/\text{s}$
P_v	Evaporative heat flux, $\text{J/m}^2/\text{s}$
$Q_{Di \text{ min}}$	Minimum distillate flow rate which allows maintaining ΔT of $T_{Fa} - T_{Da}$
Q_F	Feed flow rate applied in the simulation, m^3/s
Q_C	Recycling flow rate applied in the feed compartment allowing having a Re_f of 2000, m^3/s
r	Nominal pore size, m
R	Universal gas constant, J/molK
r_1	Fiber inner radius, m
r_2	Fiber outer radius, m
Re_f	Reynolds number of feed
S	Required membrane area, m^2
S_e	Area of external heat exchanger, m^2
S_{fiber}	Membrane area of a fiber, m^2
T	Average membrane temperature, K
T_{ci}	Cold fluid temperature at the external heat exchanger inlet, K
T_{co}	Cold fluid temperature at the outlet of the heat exchanger, K
T_{Da}	Distillate temperature in the compartment and at module outlet, K
T_{Di}	Distillate temperature at module inlet, K
T_{Dm}	Distillate temperature at membrane surface, K
T_{Fa}	Feed temperature in the compartment, at module inlet and outlet, K
T_{Fini}	Initial feed temperature, K

T_{Fm}	Feed temperature at membrane surface, K
T_{hi}	Hot fluid temperature at the inlet of the heat exchanger, K
T_{ho}	Hot fluid temperature at the outlet of the heat exchanger, K
$W_{c \text{ tot}}$	Total conductive heat flux transferred through membrane pores per cubic meter distillate, kWh/m^3
W_{external}	External energy consumption per cubic meter distillate, kWh/m^3
W_{internal}	Internal energy requirement per m^3 of distillate, kWh/m^3
W_v	Evaporative heat flux transferred through membrane per cubic meter distillate, kWh/m^3

Greek letters

δ_m	Membrane thickness, m
γ	Membrane thermal conductivity, W/mK
ε	Porosity
ρ_F	Feed density, kg/m^3
ρ_{Di}	Distillate density at the module inlet, kg/m^3
ρ_{Do}	Distillate density at the module outlet, kg/m^3
ρ_r	Retentate density, kg/m^3
φ	Recovery rate
λ	Mean free path of water vapors, m
τ	Tortuosity factor
ΔT	Temperature difference between feed and permeate sides, K or $^{\circ}\text{C}$

be quantified. The major contribution in specific water cost through MD comes from energy demand of the process (Alobaidani et al., 2008). While continuous improvements in membrane fabrication and process design are being made, net specific energy demands (kWh of energy per unit volume of produced distillate) of the process by using existing membranes under realistic process conditions (degree of temperature polarization and efficiency of energy recovery system) is still ambiguous. The question of the energy demand of MD has been addressed both from the theoretical and experimental points of view by various authors (Summers et al., 2012; Zuo et al., 2011; Saffarini et al., 2012). Compared to other optimized processes producing water of high purity, such as multi effect distillation or reverse osmosis, the energy demand in MD remains quite high, but it can be operated with low-tech equipment compared to RO for example, and is workable in some conditions for which RO would be inefficient, such as the extraction of water from concentrated brines. The literature on MD shows a large dispersion in specific energy demand and in the corresponding specific cost of the produced water (Khayet, 2013). For a given configuration, the dispersion in energy demand of MD systems has been mainly attributed to the membrane used, different but non-optimized operating conditions applied, plant capacity, implementation of energy recovery devices such as heat exchangers, module dimensions, fouling issues etc. (Criscuoli and Drioli, 1999; Harasimowicz and Chmielewski, 1999; Cabassud and Wirth, 2003; Koschikowski et al., 2003). Khayet (2013) has extensively discussed the quite wide dispersion of published data on the energy consumption, herein named specific energy, and showed that it is extremely difficult to figure out the actual energy required to operate a MD system. We observe that, unlike for many other separation processes, the figures reported in most studies do not refer to the actual recovery rate of the process; i.e. to the amount of distilled water which can be produced out of a given amount of feed water (Table 1).

The objective of the current work was then to provide an analysis of the energy demand of DCMD including the recovery rate together with other common variables such as membrane characteristics, temperature polarization and option of using an energy recovery device.

Table 1 – Specific energy consumption (SEC) of MD mentioned in various studies.

Configuration	Membrane characteristics	Operating conditions		Feed type	SEC (kWh/m ³)	Plant capacity (m ³ /h)	Refs.
		T _f (°C)	T _p (°C)				
DCMD	Spiral wound PTFE (SEP GmbH), Pore size 0.2 μ, porosity 80%	35–80	5–30	Radioactive solution	600–1600	0.05	Harasimowicz and Chmielewski (1999)
AGMD	PTFE, Pore size 0.2 μ	60–85	–	Seawater	140–200	0.2–20	
AGMD		313–343		Brackish water	30.8		Bouguecha et al. (2005)
AGMD	PTFE, Pore size 0.2 μ, porosity 80%	–		Seawater	200–300	3.46–19	Banat et al. (2007)
DCMD in hybrid systems	PP moduels from Microdyn Nadir, Pore size 0.2 μ, porosity 73%	–	–	Seawater	1.6–27.5	931 (overall)	Macedonio et al. (2007)
DCMD	Commercfial membranes from Membrana with Pore size 0.2 μ and thickness 91 μ	39.8–59	13.4–14.4	Distilled water	3550–4580	–	Criscuoli et al. (2008)
VMD	PP, thickness 35 μ, Pore size 0.1 μ	15–22 ^a		Underground water	8100.8–9089.5	2.67–6.94	Wang et al. (2009)
PGMD	n.p	60–80		Seawater	200–360	0.007–0.02	Raluy et al. (2012)
AGMD	LDPE, thickness 76 μ, Pore size 0.3 mμ, porosity 85%, Am 7.4 m ²	50–70		Tap water, synthetic seawater	~65 to ~127	0.0034–0.0094	Duong et al. (2016)
VMD	Flat sheet PP, thickness 400 μm, Pore size 0.1 μ, porosity 70%, Am 5 m ²	80		Distilled water	130		Criscuoli et al. (2013)
DCMD	PVDF hollow fiber, thickness 240 μm	80	30	Simulated reverse osmosis brine	~130 to 1700		Guan et al. (2014)
DCMD	PTFE with PP support, mean pore size 0.5 ± 0.08, porosity 91 ± 0.5, active layer thickness 46 ± 1 μm, Am 0.67 m ²	60	18–21	Wastewater	1500	3.85	Dow et al. (2016)
DCMD	Several commercial membranes with different characteristics	85	20	Seawater	~697 to 10,457 ^b		Ali et al. (2012)

VMD—vacuum membrane distillation.

AGMD—air gap membrane distillation.

^a Mean feed temperature obtained through solar collectors.

^b Calculated from GOR data.

The optimum operating conditions in terms of energy demand and membrane area requirements have also been identified. The effect of membrane characteristics has been assessed by considering two membranes i) a commercially available membrane (Accurel, Polypropylene) originally made for gas/liquid contacting purposes but widely used for MD experiments and ii) a lab made PVDF membrane specifically developed for MD applications and precisely described in the literature (Yang et al., 2011b). The Accurel membrane can be considered as a reference since it is commercially available, whereas the other one which has been developed specifically for membrane distillation has very good performances and can be considered as an achievable target for a company willing to develop new MD membranes. The effect of temperature polarization (and therefore of hydrodynamic conditions) has been incorporated by assuming a fixed temperature polarization (here of 5 °C) on both feed and permeate sides at different feed and permeate temperatures.

2. Materials and methods

2.1. Membrane characteristics

In this work, we consider two types of hollow fiber membranes: a commercial PP membrane from Membrana (Accurel™ PP S6/2) and a PVDF membrane developed on purpose by the group of Fane and Wang and described in Yang et al. (2011b). The characteristics of both membranes and module dimensions are given in Table 2. The Accurel™ membrane was not designed for MD but is commercially available and technically compatible with the requirements of MD (porous, hydrophobic polymer matrix). Surprisingly, the liquid entry pressure for the Accurel (140 kPa) is higher than the one claimed by the authors of the PVDF (138 kPa), whereas the nominal pore sizes are in an opposite ratio (0.55 versus 0.41 respectively). We assumed that this can be explained by the difference in contact angles between water and the material the two membranes are made of (polypropylene and PVDF) and by the prospective surface treatments these may have been submitted to.

2.2. Description of the simulated system

The system considered in the present study is shown diagrammatically in Figs. 1 and 2. We will assume that it processes 1 m³/h of feed flow and that it produces a flow φ m³/h of distilled water, φ then being the recovery rate for the system. The system is fitted with a hollow fiber membrane module. Heat can be supplied to the membrane module so as to compensate the heat losses through the membranes. When a heat exchanger is considered, two possible arrangements are considered, whether the heat exchanger is located on the distillate line (Fig. 1) or on the retentate line (Fig. 2). If the feed stream is available at ambient temperature, preheating is then necessary before entering the DCMD module at temperature $T_{F,a}$. On the other side, we assume that the distillate compartment, which needs to be kept at a low temperature, is circulated with a distillate stream entering the module (on the shell-side) at ambient temperature $T_{D,i}$ which is set for the purpose of our modeling at 20 °C. This stream is warmed during the process by the conductive and condensation heat fluxes to a temperature $T_{D,a}$. The outlet distillate temperature has to be lower than the inlet feed one, $T_{F,a}$. The power to maintain a low temperature in this compartment is often overlooked in technical studies. In the present work, we use the flow that need to be pumped through the distillate compartment as an indicator to reflect the need for cooling the system. In practice, the cooling

of distillate stream could be achieved by using a heat pump, though in general quite an expensive option.

The detailed conditions considered for simulation are provided in Table 2.

2.2.1. Axial and radial temperature distribution in a DCMD module

Temperature and temperature differences across the membranes are key parameters in a DCMD module. We have developed a model to simulate the local temperature difference in the radial direction across the hollow fiber section as well as in the axial direction, so as to define in which operating conditions the temperature gradients in both directions should be accounted for and those where it can be neglected. The model is based upon application of simultaneous heat and mass balance on differential elements along the fiber to determine temperature and flux profiles. The details on the model derivation and its validation for PP membrane considered in the present study have been given elsewhere (Ali et al., 2016a,b).

2.2.2. Limiting conditions and hypothesis

In this part of our work, we consider flow conditions such that the feed and distillate cross flows are high enough for the temperatures to be constant all along the module length. The permeate temperature at the module inlet ($T_{D,i}$) is set at 20 °C while the permeate temperature at the module outlet is equal to the average temperature in the permeate compartment ($T_{D,a}$) assumed ideally mixed. On the feed side, a heating system is needed to keep the temperature at a set value. Here again, we assume that the feed compartment is well mixed along the fiber axis. Evaporation of the solvent on the feed side and condensation on the distillate side combined with conduction through the membrane can create a temperature gradient in the direction radial to the main flow ("temperature polarization").

In order to incorporate a possible effect of temperature polarization to the present study, a preliminary evaluation of such temperature differences was made using a model developed by one of us (Ali et al., 2016a). The results reported in Appendix A show that in our conditions and for the membranes considered, this difference was never larger than 4 K either on the permeate and feed side. Therefore, in order to evaluate the effect of temperature polarization far from ideal conditions, we assumed a difference between the bulk and the wall temperature is 5 °C on either side (Table 3):

$$T_{F,m} - T_{F,a} = -5 \text{ °C}$$

$$T_{D,m} - T_{D,a} = +5 \text{ °C}$$

2.3. Modelling procedure

2.3.1. Membrane module analysis

Flux in MD can be described with the following equation.

$$J_w = B(P_{Fm} - P_{Dm}) \quad (1)$$

where P_{Fm} and P_{Dm} are vapor pressures at the membrane surface on feed and permeate sides, respectively. B is the distillation coefficient of the membrane (i.e. membrane permeability). Calculation of B depends mainly upon the membrane characteristics. B can be calculated using a Knudsen diffusion model (Eq. (2)) if $r < 0.5\lambda$, where r and λ represent

Table 2 – Main properties of the membranes considered in current study.

Fiber inner radius (r_1)	0.9/0.46	mm
Fiber outer radius (r_2)	1.3/0.735	mm
Membrane thickness (δ_m)	0.4/0.275	mm
Nominal pore size (r)	0.22/0.0641	μm
Maximum pore size	0.55/0.421	μm
LEP values determined for the largest pores of membranes	140 (Macedonio et al., 2014)/138	kPa
Membrane thermal conductivity (γ)	0.08/0.05	W/K m
Porosity (ϵ)	73/85	%
Hollow fiber length applied in the simulation (L)	1/1	m
Membrane characteristic parameter (B)	$8.81 \times 10^{-8}/1.31 \times 10^{-7}$	

1st and 2nd numbers in each pair represent PP and PVDF membrane, respectively.

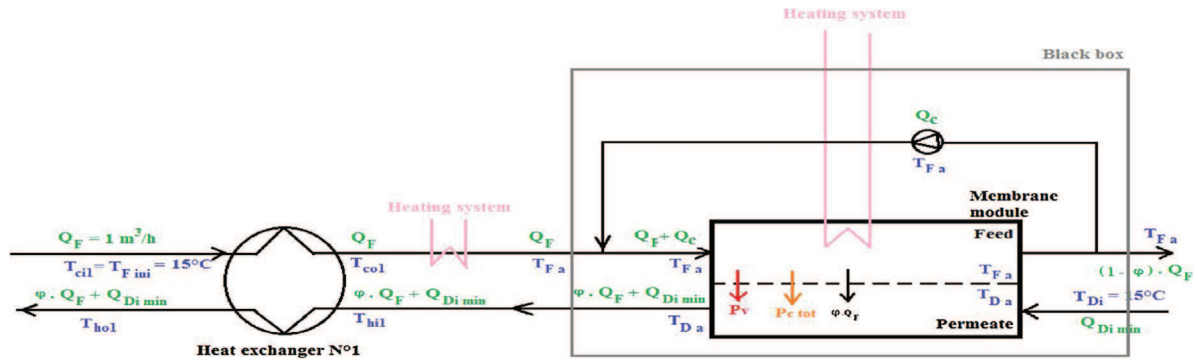


Fig. 1 – First simplified flowsheet of membrane distillation system connected to an external heat exchanger on distillate stream and to an internal energy source inside the membrane module.

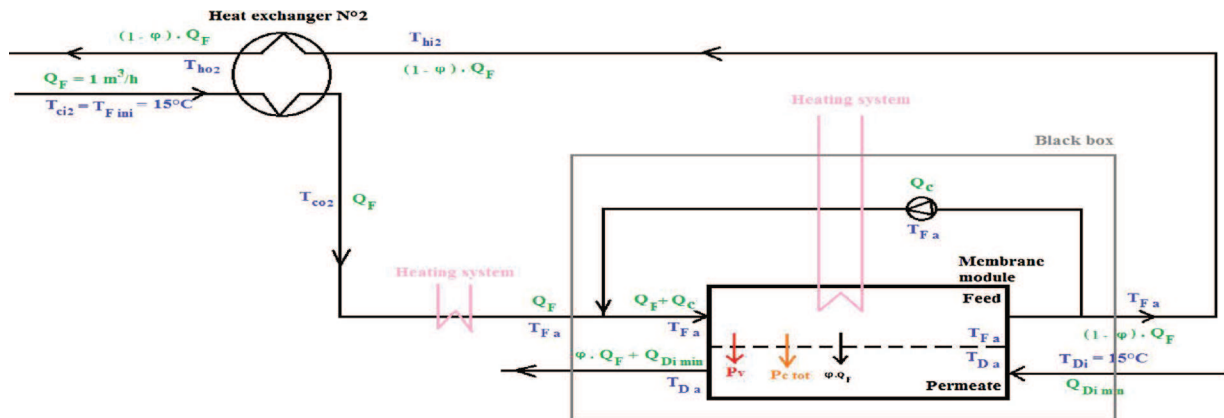


Fig. 2 – Second simplified flowsheet of membrane distillation system connected to an external heat exchanger on retentate stream and to an internal energy source in the membrane module.

Table 3 – Thermal conditions considered in current study.

DCMD system assuming no temperature polarization											
T_{Da} ($^\circ\text{C}$)	T_{Dm} ($^\circ\text{C}$)	ΔT (K or $^\circ\text{C}$)	T_{Fa} ($^\circ\text{C}$)	T_{Fm} ($^\circ\text{C}$)	T_{Di} ($^\circ\text{C}$)	T_{Fini} ($^\circ\text{C}$)	C_{pDi} (J/K kg)	C_{pDo} (J/K kg)	ρ_{Di} (kg/m ³)	ρ_{Do} (kg/m ³)	
20	20	15	35	35	20	20	4164	4158	999	998	
35	35		50	50				4147		995	
45	45		60	60				4144		993	
65	65		80	80				4144		989	
DCMD system with the presence of temperature polarization											
T_{Da} ($^\circ\text{C}$)	T_{Dm} ($^\circ\text{C}$)	ΔT (K or $^\circ\text{C}$)	T_{Fa} ($^\circ\text{C}$)	T_{Fm} ($^\circ\text{C}$)	T_{Di} ($^\circ\text{C}$)	T_{Fini} ($^\circ\text{C}$)	C_{pDi} (J/K kg)	C_{pDo} (J/K kg)	ρ_{Di} (kg/m ³)	ρ_{Do} (kg/m ³)	
20	25	5	35	30	20	20	4164	4158	999	998	
35	40		50	45				4147		995	
45	50		60	55				4144		993	
65	70		80	75				4144		989	

mean pore size and mean free path of water vapors, respectively (Khayet, 2011). λ can be calculated by using Eq. (2):

$$\lambda = \frac{k_B T}{\sqrt{2\pi P_{avg}} \sigma^2} \quad (2)$$

where k_B , P_{avg} and σ represents the Boltzmann constant, the mean pressure inside the membrane pore and the collision diameter (2.641 Å for water vapor), respectively.

$$B_k = \frac{2}{3RT} \frac{\varepsilon r}{\tau \delta} \left(\frac{8RT}{\pi M} \right)^{1/2} \quad (3)$$

In the range, $0.5\lambda < r < 50\lambda$, B can be calculated using a Knudsen-molecular diffusion model (Khayet, 2011) (Eq. (4)):

$$B = \left[\frac{3\tau\delta_m}{2\varepsilon r} \left(\frac{\pi RT}{8M} \right)^{1/2} + \frac{\tau\delta_m}{\varepsilon} \frac{Pa}{PD} \frac{RT}{M} \right]^{-1} \quad (4)$$

Where $PD = 1.895 \times 10^{-5} \times (T)^{2.072}$
 $Pa = 101325 \text{ Pa}$

B is slightly dependent on the experimental conditions. B was calculated in each case considered in our work by using the data provided in Table 2 and Eqs. (2)–(4).

The relationship between the water vapor pressure and the temperature is given by the Antoine equation (Banat et al., 2007):

$$P_{Fm/Dm} = \exp \left(23.2 - \frac{3816.44}{(T_{Fm/Dm} + 273.15) - 46.13} \right) \quad (5)$$

T_{Fm} [°C] and T_{Dm} [°C] are the feed and permeate temperatures at the membrane surface, respectively.

The water flux J_w can be obtained by combining Eqs. (1), (3)–(5) and the required membrane area S can be calculated as follows:

$$S = \frac{Q_F \times \varphi \times 1000}{J_w} \quad (6)$$

The total heat flux through the membrane, P_{tot} , is governed by two mechanisms: 1) conduction across the membrane material and its gas filled pores (P_{ctot}), and 2) latent heat associated to the water vapor molecules (P_v). Therefore, the net heat flux transported through the membrane can be expressed as follows:

$$P_{tot} = P_{ctot} + P_v \quad (7)$$

The enthalpy balance on the feed compartment is:

$$Q_F \cdot \rho_F \cdot C_{pF} \cdot T_{Fa} + P_{internal} = (1 - \varphi) \cdot Q_F \cdot \rho_r \cdot C_{pr} \cdot T_{Fa} + P_{ctot} + P_v \quad (8)$$

where P_{ctot} , P_v and $P_{internal}$ are the total conductive heat flux, evaporative heat flux and power to be supplied to the membrane module in Watt, respectively. ρ_F and ρ_r refer to the feed and retentate densities in kg/m³. C_{pF} and C_{pr} denote the feed and retentate specific heats in J/kg. K. Q_F is equal to 1 m³/h in the present simulation. φ notifies the recovery rate.

Identically, the heat balance on the distillate side is given by Eq. (9):

$$(Q_{Di \min} \cdot C_{pDi} \cdot \rho_{Di} \cdot T_{Di}) + P_{ctot} + P_v = (Q_{Di \min}$$

$$+ \varphi \cdot Q_F) \cdot C_{pDo} \cdot \rho_{Do} \cdot T_{Da} \quad (9)$$

T_{Di} and T_{Da} represent the distillate temperatures at the module inlet and outlet. C_{pDi} , C_{pDo} , ρ_{Di} and ρ_{Do} indicate the distillate specific heats and the distillate densities at the membrane inlet and outlet, respectively. The mass flux transferred through the membrane equals to $\varphi \cdot Q_F$. The minimum distillate flow rate ($Q_{Di \min}$) which allows maintaining ΔT of $T_{Fa} - T_{Da}$ is calculated by solving Eq. (9).

The latent heat flux (P_v) used in Eq. (9) for dilute solutions is determined by:

$$P_v = \varphi \cdot Q_F \cdot \rho_F \cdot H_v \quad (10)$$

The heat of evaporation is transferred to the distillate by condensation. The heat of vaporization varies upon the evaporating water temperature. In the range of temperature 273–373 K, water latent heat of vaporization is expressed as below (Phattaranawik et al., 2001):

$$H_v\{T\} = 1.7535 \cdot T_{Fm} + 2024.3 \quad (11)$$

H_v and T_{Fm} are in kJ/kg and K, respectively. The evaporative heat flux transferred through the membrane per cubic meter of produced distillate, W_v [kWh/m³] is defined as:

$$W_v = \frac{P_v}{\varphi \cdot Q_F} \quad (12)$$

For one hollow fiber of length L, internal radius r_1 and external radius r_2 , the conductive heat flux can be calculated by (Cengel, 2002):

$$P_{c \text{ fiber}} = \frac{2\pi \cdot \gamma \cdot \Delta T \cdot L \cdot (r_2 - r_1)}{\delta_m \cdot \ln \frac{r_2}{r_1}} \quad (13)$$

where γ [W/m K] is the thermal conductivity of the membrane used. ΔT is the temperature difference between feed and permeate sides. Various models have been considered to calculate γ . In general the following expression is used (Raluay et al., 2012):

$$\gamma = \varepsilon \cdot k_g + (1 - \varepsilon) \cdot k_p \quad (14)$$

where k_p is the thermal conductivity of the material forming the membrane matrix and k_g is the thermal conductivity of the gas filling the membrane pores.

The membrane surface area of a fiber is determined as below:

$$S_{\text{fiber}} = 2\pi \cdot r_1 \cdot L \quad (15)$$

Knowing the membrane area (S) from Eq. (6) and membrane area of a fiber (S_{fiber}), the number of hollow fibers required (N_{fiber}) is found by combining Eqs. (6) and (15):

$$N_{\text{fiber}} = \frac{S}{S_{\text{fiber}}} \quad (16)$$

Therefore, the total conductive heat flux (P_{ctot} in Watt) is obtained by combining Eqs. (13) and (16):

$$P_{ctot} = P_{c \text{ fiber}} \cdot N_{\text{fiber}} \quad (17)$$

The total conductive heat flux transferred through the membrane pores per cubic meter of distillate, W_{ctot} [kWh/m³] is determined by:

$$W_{ctot} = \frac{P_{ctot}}{\varphi \cdot Q_F} \quad (18)$$

A DCMD module needs to be heated in order to compensate the heat loss by conduction and evaporation and to keep a preset average feed temperature (T_{Fa}). For a given inlet feed temperature and a determined recovery rate, this energy requirement per m³ of distillate, $W_{internal}$ [kWh/m³] is defined as below:

$$W_{internal} = \frac{(1 - \varphi) \cdot Q_F \cdot \rho_r \cdot C_{pr} \cdot T_{Fa} + P_{ctot} + P_v - Q_F \cdot \rho_F \cdot C_{pF} \cdot T_{Fa}}{\varphi \cdot Q_F} \quad (19)$$

Some preheating energy has to be supplied to the feed in order to reach the desired temperature at the module inlet (T_{Fa}). For the DCMD system assuming no external heat exchanger, the external energy consumption per cubic meter of produce distillate is obtained by:

$$W_{external\ without\ exchanger} = \frac{Q_F \cdot \rho_F \cdot C_{pF} \cdot (T_{Fa} - T_{Fini})}{\varphi \cdot Q_F} \quad (20)$$

An average outdoor temperature of 20 °C is assumed. In this case (without external heat exchanger), $T_{Fini} = T_{co} = 20$ °C. The preheating energy supplied to the feed is changed when an external heat exchanger is added to the membrane distillation system. The preheating energy required in the presence of a heat exchanger is defined as below:

$$W_{external\ with\ exchanger} = \frac{Q_F \cdot \rho_F \cdot C_{pF} \cdot (T_{Fa} - T_{co})}{\varphi \cdot Q_F} \quad (21)$$

where T_{co} denotes the cold fluid temperature at the outlet of the heat exchanger used.

The specific energy consumption per cubic meter distillate, E_p [kWh/m³] is simply obtained by:

$$E_p = W_{external} + W_{internal} \quad (22)$$

2.3.2. Heat exchanger

Many descriptions of DCMD involve the use of heat exchangers in order to recover part of the spare heat available in the streams flowing out of the MD unit and discuss their interest. We therefore have considered this option and assumed that we could use it either on the retentate or on the distillate line. We have considered various surface areas for the heat exchangers adapted to the flow to be handled. The main design equations used for calculating the heat recovered through this device are presented in [Appendix A](#).

3. Result and discussion

3.1. Identification of set conditions

A variation of temperature along and across the flow area is expected in MD due to heat and mass transfer. To identify the conditions under which the assumption of the variation in temperature along the module holds true, temperature profiles on feed and permeate sides were obtained under various

temperature and hydrodynamic conditions. As expected, the temperature distribution along the fiber becomes more uniform with an increase in feed flow rate for any combination of feed and permeate temperatures. However, it was noted that for low feed temperatures, it is relatively easy to achieve the conditions under which the temperature distribution in axial direction can be approximated uniform. Bulk and surface profiles along the fiber corresponding to feed and permeate inlet temperatures of 308.15 K and 293.15 K, respectively are shown in [Fig. 3\(a\)](#) and for feed and permeate inlet temperatures of 333.15 K and 318.15 K in [Fig. 3\(b\)](#). Feed and permeate velocities are kept at 2.5 and 3 m/s respectively for these conditions. It can be noticed that the average temperature polarization both on feed and permeate sides remains less than 2 K under these conditions. In our calculation and in order to consider a worse case situation, the effect of temperature polarization was incorporated by considering its value of 5 K on each side.

3.2. Flux

The flux calculated for PP and PVDF membranes according to the model described in Section 2.3.1 is shown in [Fig. 4](#). Knudsen-molecular and Knudsen diffusion model was applied for PP and PVDF membrane respectively in accordance with the conditions mentioned in Section 2.2.2. The water flux transferred through the membrane pores is proportional to the partial pressure difference and as expected, it is much lower whatever the recovery rate and membrane type, when considering a temperature polarization of 5 °C (Eq. (1)). The increase in water flux at a higher average feed temperature is well known and is due to the increase in partial pressure difference (Eqs. (1) and (5)) even if the temperature difference between the two compartments is assumed constant at 15 °C. The PVDF membrane would produce a 73% higher flux than the PP one.

In the case of a saline solution, the water vapor pressure would change with the salt concentration. The following correlation has been proposed to reflect the effect of salt concentration on water vapor pressure ([Yun et al., 2006](#)):

$$P = P^0 (1 - x) \quad 1 - 0.5x - 10x^2 \quad (23)$$

where P^0 is the vapor pressure of pure water and x is the mole fraction of NaCl in solution. In the case of a reverse osmosis brine (c.a. 75 g/L) concentrated by MD up to 110 g/L, i.e. ≈ 2 M in NaCl, the mole fraction of NaCl would be ≈ 0.04 . According to Eq. (23), the vapor pressure would be only 8% lower than for pure water. The impact on the actual mass flux (8%) is quite limited compared to the broad variation in sodium chloride concentration from 0 to 110 g/L.

3.3. Membrane area

The membrane area requirement increases linearly with the recovery rate and can be very large as soon as the recovery exceeds 10–20%. Whatever the membrane type, a high feed temperature (T_{Fa}) is essential to keep the required membrane area to reasonable levels ([Figs. 5 and 6](#)).

These values of membrane area are however huge and clearly indicate the need for process improvement in terms of less temperature polarization and the development of high performance membranes specifically developed for MD (low conductivity and high flux), as long as significant recovery rates are expected.

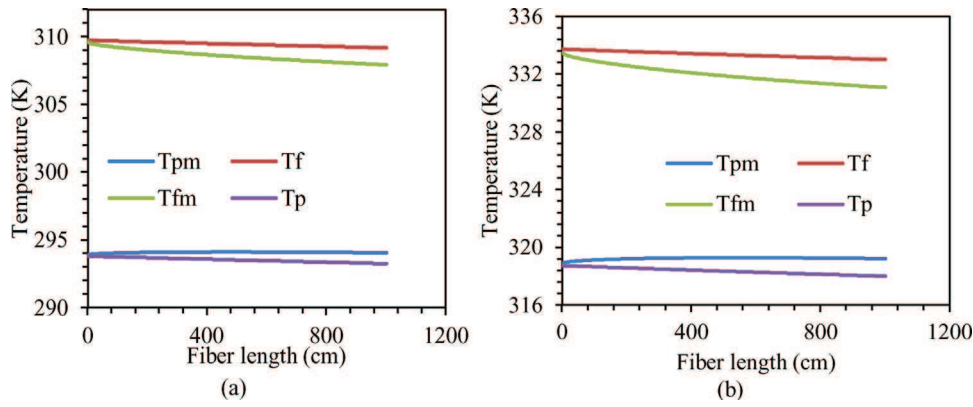


Fig. 3 – Temperature distribution on feed and permeate sides for corresponding stream velocities of 2.5 and 3 m/s, respectively.

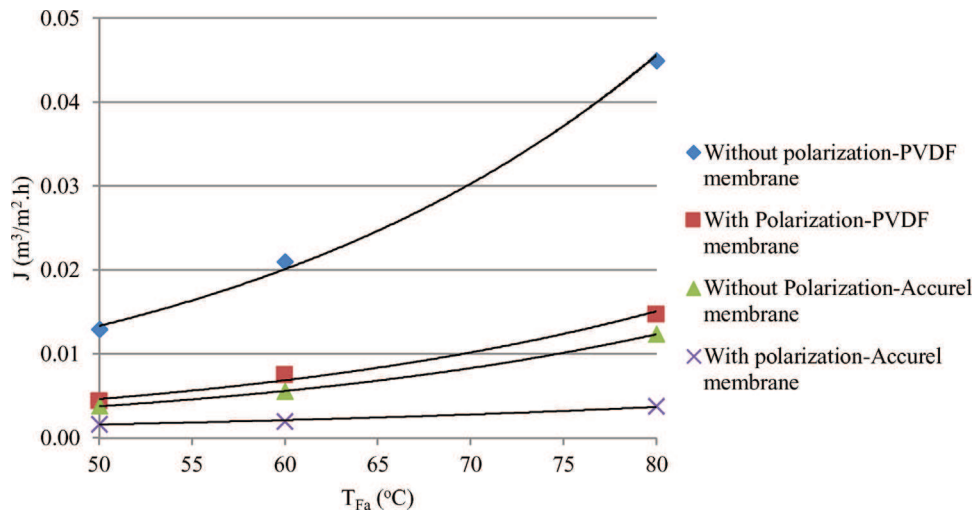


Fig. 4 – Water flux transferred through the membrane as a function of average feed temperature for DCMD systems assuming no temperature polarization/with the presence of temperature polarization and operating with Accurel membrane/PVDF membrane ($Q_F = 1 \text{ m}^3/\text{h}$, $T_{Di} = 20^{\circ}\text{C}$, $T_{Da} = T_{Fa} - 15^{\circ}\text{C}$).

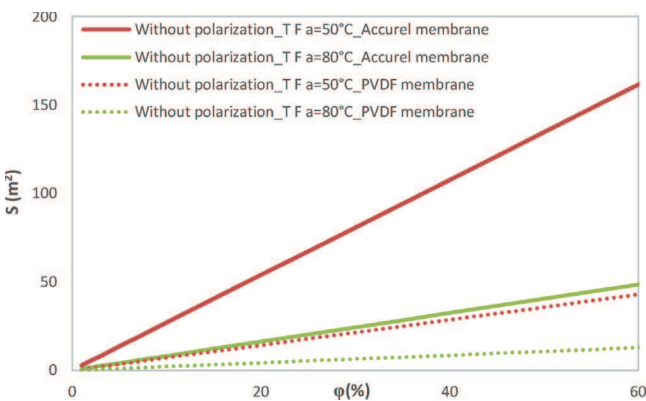


Fig. 5 – Membrane area as a function of recovery rate for DCMD systems assuming no temperature polarization and operating with PP membrane/PVDF membrane at 2 average feed temperatures ($Q_F = 1 \text{ m}^3/\text{h}$).

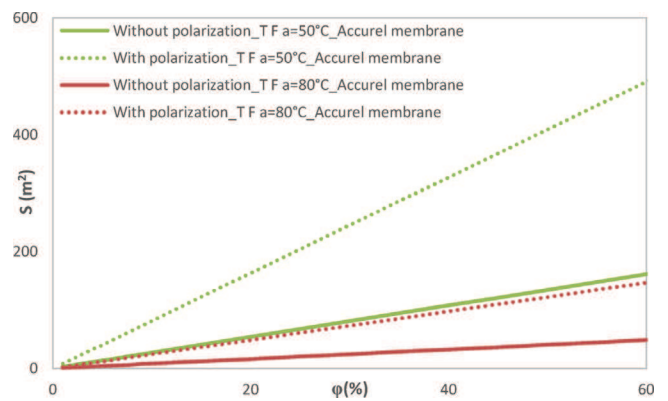


Fig. 6 – Membrane area as a function of recovery rate for DCMD systems assuming no temperature polarization/with the presence of temperature polarization and operating with PP membrane at 2 average feed temperatures ($Q_F = 1 \text{ m}^3/\text{h}$).

3.4. Minimum distillate flow rate

The minimum permeate flow rate ($Q_{Di,min}$) which allows maintaining a given average temperature difference between the feed and permeate sides is determined by solving Eq. (9).

The minimum distillate flow rate (which is an indicator of the amount of energy that would be needed to cool the distillate compartment) increases with the recovery rate because of

higher heat flux transferred through the membrane. It is much reduced (85–78% smaller) when the feed average temperature is increased from 50 $^{\circ}\text{C}$ to 80 $^{\circ}\text{C}$, and this is directly linked to the smaller surface area needed at this higher temperature and to a latent heat which is only slightly changed. The part played by the temperature polarization is interesting since it appears that the system needs the same distillate flow rate whether

the temperature polarization is considered or not. In fact, for a given recovery rate, the transfer of latent heat is almost the same whether polarization is important or not. As described in Eq. (13), the heat transported by conduction depends on the product of the difference in temperature by the membrane area. The effect of the temperature polarization is to decrease the former and increase the latter, both effects compensating each other here.

In any case, keeping the distillate compartment at a reasonably low temperature compared to the feed temperature would need unrealistic volumes of cool water (or their equivalent in electric power to operate a heat pump) unless the feed stream is maintained at quite a high temperature and, of course, the membrane used is a high performance one. Therefore, cooling the distillate compartment can be one of the factors limiting the recovery rate when operating a DCMD unit, though this aspect of the process is often overlooked in the literature.

3.5. Specific energy

3.5.1. System without external heat exchanger

For a given average feed temperature (T_{Fa}), the energy needed to be kept the feed compartment at a desired temperature decreases with the increase in T_{Fa} but increases slightly when in the presence of temperature polarization because of a higher conductive heat flux (Fig. 8). Working with a higher performance membrane, the system needs less internal energy due to the reduction in conductive flux.

The total specific energy (Eq. (22)) plotted as a function of recovery rate gives curves which are typically represented in Fig. 9.

The specific energy demand decreases with the increase in average feed temperature as expected, except at very low recovery rate. The horizontal lines represent W_{int} , and by comparison to the dotted lines, one can appreciate the cost of preheating the feed to a given temperature as a function of the recovery rate. The specific energy decreases sharply with the recovery rate at low values of the latter because in this range, the energy to warm the whole stream from ambient temperature to the module inlet temperature is a significant fraction of the total energy requirement. For large recovery rates, this specific energy demand remains almost constant. The result shows that the temperature polarization for a given recovery rate has almost no impact on the overall energetic performance because to produce a given quantity of distillate (a given recovery rate), the increase in membrane surface nearly compensates the temperature difference in generating conductive heat flux. As expected, the DCMD system requires much less specific energy when a high performance membrane is used. This is due to the reduction in conductive heat flux. The results presented in Fig. 9 show that for an energy point of view, preheating the feed at a relatively high temperature provides a much better yield provided that the recovery rate exceeds 10% or so.

Figs. 7 and 10 illustrate that the system needs less minimum distillate flow rate and less membrane area (i.e. less investment cost) at low recovery rate. On another hand, the higher the recovery rate, the lower the specific energy requirement. The tradeoff obviously would depend on the cost of energy and materials and it is definitely case-specific. It is beyond the scope of the present study to set the exact operating point, but it is clear in Fig. 10 that this point drifts towards higher recovery rates for warmer feeds. As expected, the best

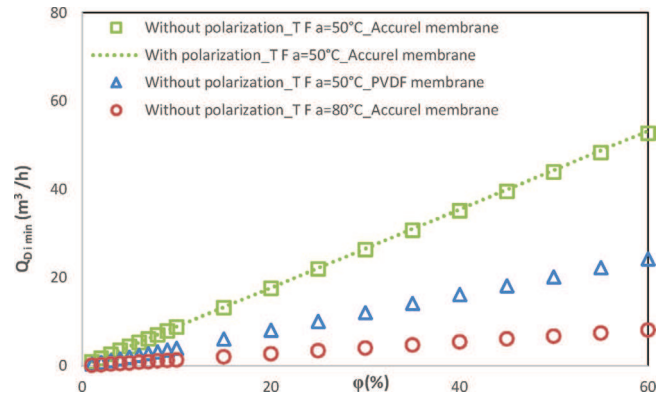


Fig. 7 – Minimum distillate flow rate as a function of recovery rate for DCMD systems assuming no temperature polarization/with the presence of temperature polarization and operating with Accurel membrane/PVDF membrane ($Q_F = 1 \text{ m}^3/\text{h}$).

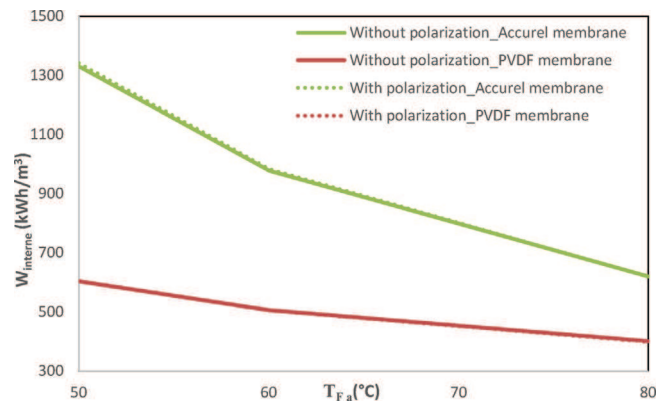


Fig. 8 – Internal energy to be supplied to the membrane module (Eq. (19)) as a function of average feed temperature for DCMD systems assuming no temperature polarization/with the presence of temperature polarization and operating with Accurel membrane/PVDF one.

operation condition is running the system at high average feed temperature.

3.5.2. System with external heat exchanger

As in any thermal process, one searches to recycle heat fluxes by using heat exchangers to transfer heat from exiting streams back to feed flows. In membrane distillation, two options (at least) can be considered: one is to connect the retentate which exits from the module to the feed stream entering the module (case n°2 in the present work) and the other one using the distillate stream to pre-heat the feed (case n°1 in the present work) and this has been described in many papers before (Lin et al., 2014; Geng et al., 2014).

As can be seen in Figs. 11 and 12, based on the flow sheets shown in Figs. 1 and 2 respectively, the impact of using a heat exchanger decreases when the recovery rate increases. A comparison between Figs. 11 and 12 clearly shows the advantage of plugging the heat exchanger on the retentate line, which enters the heat exchanger at a higher temperature than when the heat exchanger is connected to the exit of the distillate line. The flow of retentate would obviously decrease as the recovery increases, but this should not impact the final energy demand since at high recovery rate, we observe a limited impact of the presence of a heat exchanger, since as commented about Fig. 9, the part played by the pre heating energy

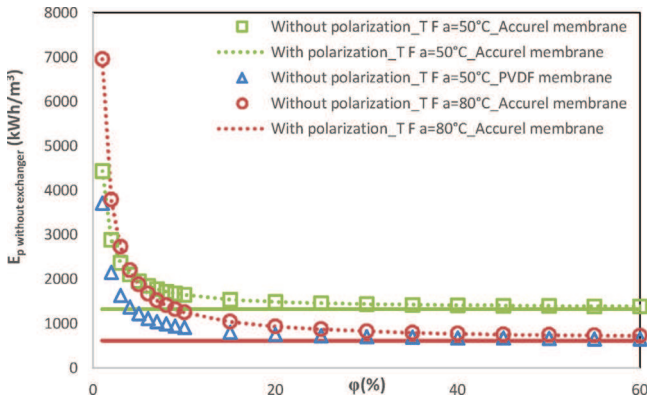


Fig. 9 – Specific energy requirement as a function of recovery rate for DCMD systems assuming no temperature polarization/with the presence of temperature polarization and operating with Accurel membrane/PVDF one at 2 average feed temperatures when an external heat exchanger is not used ($Q_F = 1 \text{ m}^3/\text{h}$).

Green and red solid lines represent the internal energies at 35°C and 80°C , respectively. (For interpretation of the references to color in this figure legend, the reader is referred to the web version of this article.)

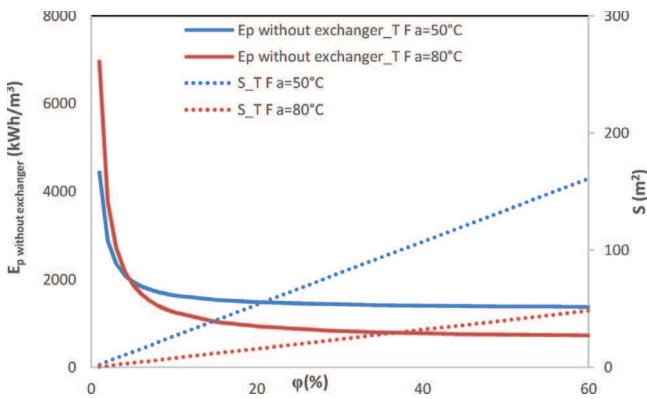


Fig. 10 – Specific energy consumption and membrane area as a function of recovery rate for DCMD assuming no temperature polarization and operating with Accurel membrane when an external heat exchanger is not used ($Q_F = 1 \text{ m}^3/\text{h}$).

on the overall specific energy fades out when the recovery increases.

The result shows that whatever T_{Fa} , the DCMD system requires less specific energy especially at very low recovery rate (61% smaller at the recovery rate of 1%) by using the external heat exchanger N°2. Therefore, it would be better to recover the heat available in the retentate stream to preheat the feed instead of in the distillate one.

Overall, the specific energy remains quite high, compared to other water distillation processes such as multistage flash distillation ($70 \text{ kWh}/\text{m}^3$) or to reverse osmosis ($3\text{--}7 \text{ kWh}/\text{m}^3$). Even when abundant sources of hot feed is available, the implementation of a heat exchanger, especially on the retentate line may prove profitable only to allow an operation at lower recovery rates, while keeping the specific energy demand low.

4. Conclusion

We have considered DCMD using a hollow fiber module coupled with an external heat exchanger, an external heating

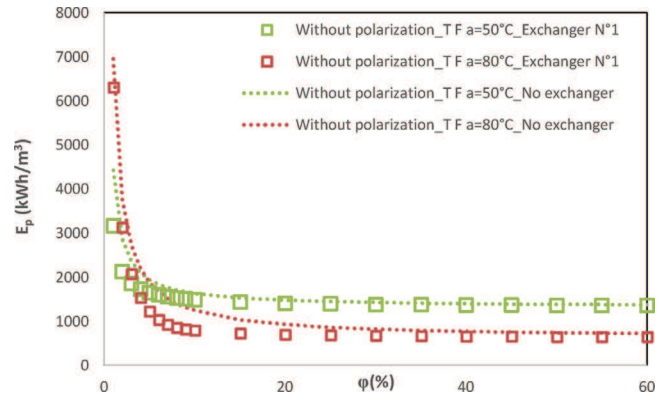


Fig. 11 – Specific energy as a function of recovery rate for DCMD systems assuming no external heat exchanger/with the external heat exchanger used to recover the heat available in the distillate stream and operating with Accurel membrane when the temperature polarization is not considered.

($S_{\text{exchanger}} = 1 \text{ m}^2$, $Q_F = 1 \text{ m}^3/\text{h}$, $T_{Da} = 35^\circ\text{C}$ and 65°C for $T_{Fa} = 50^\circ\text{C}$ and 80°C , respectively).

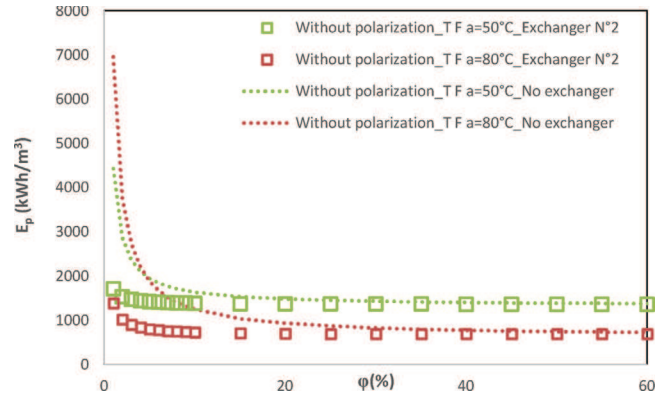


Fig. 12 – Specific energy as a function of recovery rate for DCMD systems assuming no external heat exchanger/with the external heat exchanger used to recover the heat available in the retentate stream and operating with Accurel membrane when the temperature polarization is not considered.

($S_{\text{exchanger}} = 1 \text{ m}^2$, $Q_F = 1 \text{ m}^3/\text{h}$, $T_{Da} = 35^\circ\text{C}$ and 65°C for $T_{Fa} = 50^\circ\text{C}$ and 80°C , respectively).

system and an internal energy source in the membrane module. This system is simulated in order to evaluate the thermal energy requirement as a function of the recovery rate, i.e. the ratio between the amount of distilled water produced by the amount of feed processed. The influence of the temperature polarization on the energy consumption is considered.

When considering situations where the feed stream has to be heated, we find that the specific energy required to produce a given amount of distilled water decreases sharply when the recovery rate increases from 0 to c.a. 20%. This level of specific energy obviously decreases when the DCMD is operated at high feed temperature and with a high performance membrane, as this has been pointed out in previous studies. The cost of heating the feed from ambient temperature to a higher temperature is worth the energy spent, provided that the recovery rate is high enough.

Our results show that for a given recovery rate, the specific energy requirement of DCMD is only slightly dependent on “temperature polarization”. This can be explained as TP

increases the membrane surface area needed to produce a given amount of distilled water, and at the same time decreases the temperature gradient which is the driving force for heat conduction through the membranes. In the conditions in this simulation, both phenomena balance each other almost exactly.

We also found that, under the conditions considered in current study, a heat exchanger is more efficient if implemented on the retentate line better than on the distillate. The impact of using a heat exchanger is however limited to the range of recovery rates for which the energy required for pre heating the feed is significant compared to the total energy needed by the process, i.e. in the range between 0 and 20% in our conditions.

Running the same calculations but for two different membranes allowed to appreciate that when switching from a non-optimized membrane to an optimized one, the membrane surface area necessary for a specific duty can be almost halved, whereas the role of the membrane on the energy demand is important at low recovery rates, but fades away at high recovery rates (Fig. 9).

Acknowledgments

WJ wishes to thank the Ministry of Education of Thailand and a grant from the French Embassy in Thailand; AA contribution was part of his PhD grant received from the EUDIME ITN program (Reference 2011-0014).

Appendix A. Estimation of the temperature polarization.

We used the model developed by one of us and published in [XX] to compute the temperature difference between the bulk and surface of the membrane for a range of operating conditions. The data gathered in Table A1 show that the temperature difference between the bulk and the membrane surface (subscript m) either on the feed side (subscript f) or on the permeate side (subscript D) is in a range [0.06–3.83 K].

Table A1 – Temperature.

$T_{f,in}$ (K)	$T_{p,in}$ (K)	V_f (m/s)	V_p (m/s)	$T_{D,m} - T_D$ (K) ^a	$T_f - T_{f,m}$ (K) ^a
308	293	3.13	3.13	0.06/0.15	0.25/0.46
308	293	0.13	0.13	0.69/1.09	0.74/1.49
353	338	3.13	3.13	0.23/0.53	0.97/1.63
353	338	0.13	0.13	2.07/3.83	2.21/2.84

^a 1st and 2nd value refers to PVDF and PP membranes, respectively.

Appendix B. Design of a heat exchanger.

The application of recuperative heat exchanger ensures the energy recovery from distillate and retentate leaving the module.

$$E = \frac{1 - \exp[-NUT(1-R)]}{1 - R \cdot \exp[-NUT(1-R)]} \quad \text{For } R \neq 1 \quad (24)$$

$$\text{Or } E = \frac{NUT}{NUT + 1} \quad \text{For } R = 1 \quad (25)$$

where R is the ratio of the heat capacity flows:

$$R = \frac{C_{min}}{C_{max}} = \frac{\min(Q_F \cdot \rho_F \cdot C_{pF}; (\alpha \cdot Q_F + Q_{Dimin}) \cdot \rho_{Do} \cdot C_{pDo})}{\max(Q_F \cdot \rho_F \cdot C_{pF}; (\alpha \cdot Q_F + Q_{Dimin}) \cdot \rho_{Do} \cdot C_{pDo})} \quad (26)$$

when the external heat exchanger N°1 is used,

$$R = \frac{C_{min}}{C_{max}} = \frac{\min(Q_F \cdot \rho_F \cdot C_{pF}; (1-\alpha) \cdot Q_F \cdot \rho_r \cdot C_{pr})}{\max(Q_F \cdot \rho_F \cdot C_{pF}; (1-\alpha) \cdot Q_F \cdot \rho_r \cdot C_{pr})} \quad (26\text{-bis})$$

when the external heat exchanger N°2 is used.

The number of transfer units is defined by:

$$NUT = \frac{K \cdot S_e}{C_{min}} \quad (27)$$

Knowing the efficiency of the heat exchanger, the total power exchanged (P_e) by two fluids in heat exchanger can be given by the relation:

$$P_e = E \cdot C_{min} \cdot (T_{Da} - T_{Fini}) \quad (28)$$

when the external heat exchanger N°1 is applied,

$$P_e = E \cdot C_{min} \cdot (T_{Fa} - T_{Fini}) \quad (28\text{-bis})$$

when the external heat exchanger N°2 is applied.

Also, when the external heat exchanger N°1 is applied,

$$\begin{aligned} P_e &= (\alpha \cdot Q_F + Q_{Dimin}) \cdot \rho_{Do} \cdot C_{pDo} \cdot (T_{Da} - T_{ho1}) \\ &= Q_F \cdot \rho_F \cdot C_{pF} \cdot (T_{co1} - T_{Fini}) \end{aligned} \quad (29)$$

when the external heat exchanger N°2 is applied,

$$\begin{aligned} P_e &= (1 - \alpha) \cdot Q_F \cdot \rho_r \cdot C_{pr} \cdot (T_{Fa} - T_{ho2}) \\ &= Q_F \cdot \rho_F \cdot C_{pF} \cdot (T_{co2} - T_{Fini}) \end{aligned} \quad (29\text{-bis})$$

Introducing the known values, P_e , C_p and the inlet temperatures in Eq. (29) or (29-bis), the outlet temperatures (T_{co} and T_{ho}) can be obtained. T_{co} is then applied in Eq. (21).

References

- Ali, M.I., Summers, E.K., Arafat, H.A., Lienhard V, J.H., 2012. *Effects of membrane properties on water production cost in small scale membrane distillation systems. Desalination 306, 60–71.*
- Ali, A., Macedonio, F., Drioli, E., Aljlil, S., Alharbi, O.a., 2013. *Experimental and theoretical evaluation of temperature polarization phenomenon in direct contact membrane distillation. Chem. Eng. Res. Des. 91 (October (10)), 1966–1977.*
- Ali, A., Aimar, P., Drioli, E., 2015. *Effect of module design and flow patterns on performance of membrane distillation process. Chem. Eng. J. 277, 368–377.*
- Ali, A., Quist-jensen, C.A., Macedonio, F., Drioli, E., 2016a. *Optimization of module length for continuous direct contact membrane distillation process. Chem. Eng. Process. Process Intensif. 110, 188–200.*
- Ali, A., Quist-Jensen, C.A., Macedonio, F., Drioli, E., 2016b. *On designing of membrane thickness and thermal conductivity for large scale membrane distillation modules. J. Membr. Sci. Res. 505 (May (01)), 167–173.*
- Alobaidani, S., Curcio, E., Macedonio, F., Diproffio, G., Alhinai, H., Drioli, E., 2008. *Potential of membrane distillation in seawater desalination: thermal efficiency, sensitivity study and cost estimation. J. Membr. Sci. 323 (October (1)), 85–98.*

- Banat, F., Jwaied, N., Rommel, M., Koschikowski, J., 2007. Performance evaluation of the 'large SMADES' autonomous desalination solar-driven membrane distillation plant in Aqaba, Jordan. *Desalination* 217, 17–28.
- Bouguecha, S., Hamrouni, B., Dhahbi, M., 2005. Small scale desalination pilots powered by renewable energy sources: case studies. *Desalination* 183 (May), 151–165.
- Cabassud, C., Wirth, D., 2003. Membrane distillation for water desalination: how to chose an appropriate membrane? *J. Membr. Sci.* 157 (May), 307–314.
- Cengel, Y.A., 2002. Heat conduction equation. In: *Heat Transfer A Practical Approach*, 2nd ed. McGraw-Hill Higher Education, pp. 61–126.
- Criscuoli, A., Drioli, E., 1999. Energetic and exergetic analysis of an integrated membrane desalination system. *Desalination* 124, 243–249.
- Criscuoli, A., Concetta, M., Drioli, E., 2008. Evaluation of energy requirements in membrane distillation. *Chem. Eng. Process.* 47, 1098–1105.
- Criscuoli, A., Carnevale, M.C., Drioli, E., 2013. Modeling the performance of flat and capillary membrane modules in vacuum membrane distillation. *J. Membr. Sci.* 447, 369–375.
- Dow, N., Gray, S., Li, J., Zhang, J., Ostarcevic, E., Liubinas, A., Atherton, P., Roeszler, G., Gibbs, A., Duke, M., 2016. Pilot trial of membrane distillation driven by low grade waste heat: membrane fouling and energy assessment. *Desalination* 391 (August), 30–42.
- Duong, H.C., Cooper, P., Nelemans, B., Cath, T.Y., Nghiem, L.D., 2016. Evaluating energy consumption of air gap membrane distillation for seawater desalination at pilot scale level. *Sep. Purif. Technol.* 166, 55–62.
- Geng, H., He, Q., Wu, H., Li, P., Zhang, C., Chang, H., 2014. Experimental study of hollow fiber AGMD modules with energy recovery for high saline water desalination. *Desalination* 344 (July), 55–63.
- Gryta, M., Tomaszewska, M., 1998. Heat transport in the membrane distillation process. *J. Membr. Sci.* 144 (1–2), 211–222.
- Gryta, M., Tomaszewska, M., Morawski, A.W., 1997. Membrane distillation with laminar flow. *Sep. Purif. Technol.* 11, 93–101.
- Guan, G., Yang, X., Wang, R., Field, R., Fane, A.G., 2014. Evaluation of hollow fiber-based direct contact and vacuum membrane distillation systems using aspen process simulation. *J. Membr. Sci.* 464 (August), 127–139.
- Harasimowicz, M., Chmielewski, A.G., 1999. Concentration of radioactive components in liquid low-level radioactive waste by membrane distillation. *J. Membr. Sci.* 163, 257–264.
- Khayet, M., 2011. Membranes and theoretical modeling of membrane distillation: a review. *Adv. Colloid Interface Sci.* 164 (May (1–2)), 56–88.
- Khayet, M., 2013. Solar desalination by membrane distillation: dispersion in energy consumption analysis and water production costs (a review). *Desalination* 308, 89–101.
- Koschikowski, J., Wiegghaus, M., Rommel, M., 2003. Solar thermal-driven desalination plants based on membrane distillation. *Desalination* 156 (May), 295–304.
- Lin, S., Yip, N.Y., Elimelech, M., 2014. Direct contact membrane distillation with heat recovery: thermodynamic insights from module scale modeling. *J. Membr. Sci.* 453, 498–515.
- Macedonio, F., Curcio, E., Drioli, E., 2007. Integrated membrane systems for seawater desalination: energetic and exergetic analysis, economic evaluation, experimental study. *Desalination* 203 (May), 260–276.
- Macedonio, F., Ali, A., Poerio, T., El-Sayed, E., Drioli, E., Abdel-Jawad, M., 2014. Direct contact membrane distillation for treatment of oilfield produced water. *Sep. Purif. Technol.* 126, 69–81.
- Phattaranawik, J., Jiraratananon, R., Fane, A.G., Halim, C., 2001. Mass flux enhancement using spacer filled channels in direct contact membrane distillation. *J. Membr. Sci.* 187, 193–201.
- Phattaranawik, J., Jiraratananon, R., Fane, A.G., 2003. Heat transport and membrane distillation coefficients in direct contact membrane distillation. *J. Membr. Sci.* 212, 177–193.
- Raluy, R.G., Schwantes, R., Subiela, V.J., Peñate, B., Melián, G., Betancort, J.R., 2012. Operational experience of a solar membrane distillation demonstration plant in Pozo Izquierdo-Gran Canaria Island (Spain). *Desalination* 290 (March), 1–13.
- Saffarini, R.B., Summers, E.K., Arafat, H.A., Lienhard V, J.H., 2012. Technical evaluation of stand-alone solar powered membrane distillation systems. *Desalination* 286, 332–341.
- Summers, E.K., Arafat, H.A., Lienhard V, J.H., 2012. Energy efficiency comparison of single-stage membrane distillation (MD) desalination cycles in different configurations. *Desalination* 290, 54–66.
- Tamburini, A., Pitò, P., Cipollina, A., Micale, G., Ciofalo, M., 2013. A thermochromic liquid crystals image analysis technique to investigate temperature polarization in spacer-filled channels for membrane distillation. *J. Membr. Sci.* 447 (November), 260–273.
- Wang, X., Zhang, L., Yang, H., Chen, H., 2009. Feasibility research of potable water production via solar-heated hollow fiber membrane distillation system. *Desalination* 247 (1–3), 403–411.
- Yang, X., Wang, R., Fane, A.G., 2011a. Novel designs for improving the performance of hollow fiber membrane distillation modules. *J. Membr. Sci.* 384 (1–2), 52–62.
- Yang, X., Wang, R., Shi, L., Fane, A.G., Debowski, M., 2011b. Performance improvement of PVDF hollow fiber-based membrane distillation process. *J. Membr. Sci.* 369 (March (1–2)), 437–447.
- Yun, Y., Ma, R., Zhang, W., Fane, A.G., Li, J., 2006. Direct contact membrane distillation mechanism for high concentration NaCl solutions. *Desalination* 188 (February), 251–262.
- Zuo, G., Wang, R., Field, R., Fane, A.G., 2011. Energy efficiency evaluation and economic analyses of direct contact membrane distillation system using Aspen Plus. *Desalination* 283, 237–244.